Testing for efficacy in four measures of demographic buffering

Samuel J L Gascoigne[1,*], Maja Kajin[1,2], Irem Sepil[1], Roberto Salguero-Gómez[1,3]

Main text

[1] Department of Biology, South Parks Road, University of Oxford, Oxford, United Kingdom

[2] Department of Biology, Biotechnical Faculty, University of Ljubljana, Večna pot 111, 1000 Ljubljana, Slovenia

[3] National Laboratory for Grassland & Agro-ecosystems, Lanzhou University, China

* Correspondence: samuel.gascoigne@abdn.ac.uk

Data accessibility statement: All data and code supporting these results will be made open access on Zenodo upon publication.

ORCID identifiers:

    Samuel J L Gascoigne: 0000-0002-2984-1810

    Maja Kajin: 0000-0001-9996-5897

    Irem Sepil: 0000-0002-3228-5480

    Roberto Salguero-Gómez: 0000-0002-6085-4433

ABSTRACT

Understanding population responses to variable environments is central to much of current research in population ecology and conservation biology. Environmental variability, a key component of global climate change, increases the extinction risk of species across the tree of life. Therefore, quantifying the sensitivity of populations to environmental variability is timely in the face of global climate change. A common approach to measure the impact of environmental variability on a population is by quantifying the population's capacity towards demographic buffering specifically, the population's ability to reduce the impact of environmental variability on its own growth rate. This line of work has, over the past 25 years, resulted in multiple, heterogeneous methods to quantify demographic buffering. To date, we lack clarity on which method is most appropriate, and under what conditions. To identify the best method to quantify demographic buffering, we test four methods – one correlational method, two methods using terms from Tuljapurkar's approximation and the summation of stochastic elasticities of variance ($\sum E_{a_{ij}}^{\sigma^2}$) – for their efficacy to inform conservation strategies. We compare and contrast these methods via three different tests to determine the efficacy of the methods across four integral projection models for plants representing different life histories. In the first test, we determine if the measures, structured by ontogeny, are similar or distinct by analyzing their covariance structure across the four species. In the second and third tests, we perform two counterfactual simulations to test if the measures offer insights about the populations' responses to variable environments that are better than chance. We find that the four methods significantly differ in their ability to identify and quantify demographic buffering. Furthermore, our simulations identify $\sum E_{a_{ij}}^{\sigma^2}$ as the most effective method to quantify demographic buffering. This work represents a clear example of *how* and *why* to test the metrics we infer from structured systems prior to their applications in systems of interest (*e.g.*, endangered populations). In addition, our finding that commonly used approaches to quantify demographic buffering are ineffective has broad implications for our current understanding of how natural populations are responding to climate change, and thus for effective conservation practices.

STATE OF THE ART

Increased environmental variability is a key threat to natural populations in response to global climate change (Masson-Delmotte et al., 2021; Sutherland et al., 2013). From droughts to hurricanes, environmental variability takes a variety of forms across species (Raventós et al., 2021; Rodríguez-Caro et al., 2021). However, the net effect of environmental variability on population dynamics is broadly conserved across taxa: it often leads to a reduction in a population's stochastic population growth rate (λ_s; Tuljapurkar, 1982, 1989) and consequent increases in extinction risk (May, 1973). These effects are especially concerning as global climate change is projected to increase environmental variability in regions hosting the highest biodiversity (Bathiany et al., 2018). Therefore, understanding the sensitivity of populations to environmental variability and the strategies populations use to reduce this sensitivity is critical.

Demographic buffering is often used to quantify the impact of environmental variability on population dynamics. Demographic buffering quantifies the degree to which a population's combination of demographic rates (*e.g.*, survival, growth, reproduction) reduce the impact of environmental variability on λ_s. Similar to a chemical buffer on a solution's pH, a more demographically buffered population has a combination of demographic rates that reduce the population's sensitivity to environmental variability relative to a less demographically buffered population (Gascoigne, Kajin, & Salguero-Gómez, 2023; Pfister, 1998). In turn, demographic buffering has been extensively used to infer both the sensitivity of populations to environmental variability (Hilde et al., 2020; Pfister, 1998) and the strategies populations use to reduce this sensitivity (McDonald et al., 2017). This understanding has led to a series of studies analysing the impact of climate variability on conservation measures (Colchero et al., 2021), population viability (Rodríguez-Caro et al., 2021), life histories (Morris et al., 2008) and more topics across ecology and evolutionary biology (Gascoigne, Kajin, Tuljapurkar, et al., 2023; McDonald et al., 2017; Morris & Doak, 2004; Santos et al., 2023). However, researchers

88 measure demographic buffering in numerous, different ways, as reviewed in Hilde et al.,

89 (2020).

90   Over the past 25 years, demographic buffering has taken a variety of mathematical forms

91 and interpretations. Mathematically, demographic buffering has been calculated using multiple

92 correlation and derivative based methods (Hilde et al., 2020; Santos et al., 2023). Furthermore,

93 these measures of demographic buffering have been inferred as both a population's relationship

94 to a variable environment (Rodríguez-Caro et al., 2021) and an evolved aspect of a population's

95 life history (Li & Ramula, 2015; McDonald et al., 2017). Currently, we lack a comprehensive

96 understanding of what is an *effective* measure of demographic buffering. We define "efficacy"

97 as the ability of a measure of demographic buffering to infer a population's response to a

98 variable environment. Unfortunately, previous research into demographic buffering often

99 assumes the efficacy of their methods without testing this assumption. Furthermore, out of the

100 suite of methods used to calculate demographic buffering, we do not know which measures are

101 more effective that others. In turn, to fill this gap in knowledge, we aim to test for *efficacy* in

102 measures of demographic buffering.

103   To test for efficacy in four measures of demographic buffering, we use four size-structured

104 stochastic integral projection models (IPMs; Easterling et al., 2000). Using the PADRINO

105 database (Levin et al., 2022), we simulate IPMs for four plant species with different life

106 histories. Subsequently, we calculate four well-established measures of demographic

107 buffering: one using a correlation method (Spearman's ρ: McDonald et al., 2017; Pfister, 1998),

108 two methods using terms from Tuljapurkar's approximation (V_s and $V_s + V_c$: Maldonado-

109 Chaparro et al., 2018; Tuljapurkar, 1989) and one using summed stochastic elasticities of

110 variance ($\sum E_{a_{ij}}^{\sigma^2}$: Haridas & Tuljapurkar, 2005; Morris et al., 2008; Tuljapurkar et al., 2003).

111 We test the potential differential efficacy of these four measures of demographic buffering with

112   three separate tests. In the first test, we analyzed the correlation structure of the four measures

113   of demographic buffering structured along the ontogeny (*i.e.*, the size classes in each IPM) of

114   the four species. Here, we hypothesized that (H1) different measures of demographic buffering

115   would offer different values for the same populations as the methods are parameterized using

116   dissimilar values (*e.g.*, stochastic *vs.* deterministic elasticities) and methods (*e.g.*, Spearman's

117   ρ correlation *vs.* summed products). In the second test, we stabilized (*i.e.*, fixed values as

118   constant through time) the demographic rates along the ontogeny, on size/stage increment at a

119   time, and regressed the difference in stochastic population growth rate ($\Delta\lambda_s$) against the degree

120   of buffering associated with each size class along the ontogeny. We hypothesized that (H2)

121   there is a strong negative relationship between the degree of buffering along the ontogeny and

122     $\Delta\lambda_s$ as we predicted stabilizing demographic rates to have the largest positive effect in the least

123   buffered size classes. In the third test, we elucidate whether counterfactual simulations of the

124   plant populations informed by their distributions of demographic buffering, along an ontogeny,

125   yield improved population growth relative to chance. Specifically, we collectively stabilize the

126   demographic rates of all size classes across a timeseries to varying degrees. The degree to

127   which the size class specific demographic rates were stabilized was determined by the

128   distributions of size class specific buffering, determined by each method (*i.e.*, ρ, V_s, $V_s + V_c$

129   and $\sum E_{a_{ij}}^{\sigma^2}$). To determine if these distributions offer improved information for demographic

130   rate stabilization relative to chance, we also simulated the random stabilization of demographic

131   rates along ontogeny as a control. We hypothesized that (H3) the stabilization of demographic

132   rates informed by size-class specific demographic buffering distributions would yield a

133   significantly higher $\Delta\lambda_s$ than a random stabilization of demographic rates.

134

135

METHODOLOGICAL APPROACH

To test for efficacy in measures of demographic buffering, *i.e.* the ability of natural populations to minimise the expected negative effects of environmental stochasticity (Hilde et al., 2020; Maldonado-Chaparro et al., 2018; Morris et al., 2008; Rodríguez-Caro et al., 2021), we used four different measures. Since these measures of demographic buffering are dependent on structured demographic models (*i.e.*, related to Tuljapurkar's approximation; Tuljapurkar, 1989), we used four environmentally explicit integral projection models (IPMs) to test our hypotheses.

<u>Environmentally explicit integral projection models</u>

We used four integral projection models (IPMs) from the PADRINO IPM database (Levin et al., 2022) to test for efficacy in measures of demographic buffering. IPMs are discrete-time population models that project a population structured by a continuous trait (*e.g.*, height, mass) within a finite domain [*i.e.*, from the smallest trait value (α) to the largest trait value (ω)] across time steps. An environmentally explicit IPM can be written as,

(Eq. 1) $\qquad n_{t+1}(z') = \int_{\alpha}^{\omega} K(z', z, \psi_t)\, n_t(z)\, dz$.

Here, the distribution of the continuous trait at time t [$n_t(z)$] is projected through the **K**-kernel [$K(z', z, \psi_t)$] to generate the distribution of the continuous trait at time $t + 1$ [$n_{t+1}(z')$]. The **K**-kernel represents a continuous two-dimensional surface quantifying the survival and potential change in state values of individuals between t and $t + 1$, as well as the per-capita contributions of size z individuals at time t to the occurrence of size z' individuals at time $t + 1$. In an environmentally explicit IPM, the **K**-kernel is a function of one or more time-dependent environment variables (ψ_t) (Ellner et al., 2016).

159   In our study, we simulated IPMs for four plant species with different life histories.

160   Specifically, we used IPMs for one herbaceous perennial (*Berberis thunbergii*, Merow et al.,

161   2017), two tropical perennials (*Calathea crotalifera* and *Heliconia tortuosa*, Westerband &

162   Horvitz, 2017) and one biennial (*Carlina vulgaris*, Rees & Ellner, 2009). The parameter values

163   and formulas used to construct these IPMs can be found in the supplementary materials.

164   To simulate the IPMs, we used a mesh point integration method (Easterling et al., 2000;

165   Ellner et al., 2016) which discretises the **K**-kernel into matrix form with $n \times n$ dimensions,

166   where each bin (n) can be thought of as a small, discrete size class along the life cycle of the

167   species. Since the discretised kernel mimics a matrix population model (MPM; Caswell, 2001),

168   we will discuss our methods in the form of matrix notation where the matrix is represented as

169   **A** with demographic rates a_{ij} referring to the survival-dependent changes in classes and

170   reproductive contributions of individuals in stage j toward stage i (Caswell, 2001).

171

172   <u>Tuljapurkar's approximation and measures of demographic buffering</u>

173   The metrics used to quantify demographic buffering are derived from Tuljapurkar's

174   approximation (Tuljapurkar, 1982, 1989, 1990). This approximation (Eq. 2) quantifies the

175   degree to which a population's collection of demographic rates across time contribute to its

176   long-run stochastic population growth rate.

177   (Eq. 2) $\log(\lambda_s) \approx \log(\lambda_1) - \frac{1}{2} [V_s + V_c]$.

178   The approximation is calculated by subtracting the summed impact of *temporal variance* of

179   these demographic rates (V_s, Eq. 3) and *within-time step covariance* between demographic rates

180   (V_c, Eq. 4) of demographic rates from the logged population growth rate associated with the

181   arithmetic mean matrix – *i.e.*, the MPM constructed through element-by-element arithmetic

182   means along the time series $[\log(\lambda_1)]$.

183   (Eq. 3) $V_s = \sum_{ij} e_{ij}^2 CV_{ij}^2$.

184   (Eq. 4) $V_c = \sum_{ij \neq kl} e_{ij} e_{kl} \left[\frac{\mathrm{cov}(a_{ij}, a_{kl})}{\overline{a_{ij}}\ \overline{a_{kl}}} \right]$.

185   Both V_s and V_c are calculated using the elasticities of λ_1 in response to demographic rates from

186   the mean MPM (e_{ij})[1]. Additionally, V_s measures the impact of variance using the squared

187   coefficient of variance of individual demographic rates (CV_{ij}^2), and V_c quantifies the impact of

188   the covariances between demographic rates by dividing the within-time step covariance of

189   demographic rates $[\mathrm{cov}(a_{ij}, a_{kl})]$ by the product of their means $(\overline{a_{ij}}\ \overline{a_{kl}})$.

190

191   <u>Four measures of demographic buffering</u>

192   The first measure of demographic buffering is a correlation-based approach. As illustrated by

193   Pfister (1998) – the seminal paper on demographic buffering – one strategy by which a

194   population can reduce V_s (Eq. 3) is by having a negative covariance between the elasticities of

195   population growth rate associated with the mean MPM (e_{ij}) and the temporal coefficient of

196   variance values of said demographic rates (CV_{ij}). In turn, this first measure of demographic

197   buffering (ρ) is a calculation of the covariance between e_{ij}^2 and CV_{ij}^2 [*i.e.*, $\mathrm{cov}(e_{ij}^2, CV_{ij}^2) = \rho$].

198   This negative covariance in ρ would mean that the demographic rates that proportionally vary

199   the most through time in population in fact have the least impact on the overall performance of

200   the population, as quantified elasticities of λ_1, whilst the most important demographic rates

---

[1] Elasticities quantify the *proportional* contribution of underlying demographic rates to changes in population growth rate – *i.e.*, $e_{ij} = \frac{a_{ij}}{\lambda} \frac{\partial \lambda}{\partial a_{ij}}$ (De Kroon et al., 1986).

201 would be proportionately stable over time. Out of all the possible measures of demographic

202 buffering, this correlation-based approach is the most commonly used (Hilde et al., 2020).

203   The second and third measures of demographic buffering use the values directly from

204 the second-term of Tuljapurkar's approximation. The second measure of demographic

205 buffering quantifies the impact of temporal variance in demographic rates (V_s, Eq. 3). The third

206 measure of demographic buffering sums the impact of demographic rate variance and within-

207 timestep covariance ($V_s + V_c$, Eq. 3,4).

208   The fourth measure of demographic buffering uses the summation of stochastic

209 elasticities of variance. The summation of stochastic elasticities of variance ($\sum E_{a_{ij}}^{\sigma^2}$) represents

210 the degree to which proportional increases in demographic rate variance negatively impacts λ_s.

211 In turn, we can numerically represent $\sum E_{a_{ij}}^{\sigma^2}$ as,

212 (Eq. 5) $\qquad \sum E_{a_{ij}}^{\sigma^2} = \sum \left[\frac{\text{var}(a_{ij})}{\lambda_s} * \frac{\lambda_s^{*a_{ij}} - \lambda_s}{0.00001 * \text{var}(a_{ij})} \right].$

213 As *per* Haridas & Tuljapurkar (2005), we can rewrite Tuljapurkar's approximation (Eq. 2) as,

214 (Eq. 6) $\qquad \log(\lambda_s) \approx \log(\lambda_1) - \frac{1}{2} \left[\sum E_{a_{ij}}^{\sigma^2} \right].$

215 Thus, we define the fourth measure of demographic buffering as $\sum E_{a_{ij}}^{\sigma^2}$.

216

217 <u>Testing for efficacy in measures of demographic buffering</u>

218 To test which measures of demographic buffering are effective, and the degree to which they

219 are effective, we ran three specific tests.

220   We tested H1, that the different measures of demographic buffering would offer

221 different values for the same populations, in two steps. First, we quantified the degree of

222 demographic buffering associated with each measure of all n size classes of the $n \times n$

223 discretised IPM, one size class at a time. Second, we quantified the correlation of these values

224 for all four species. If the measures of demographic buffering are distinct, different correlation

225 patterns of the measures should emerge across the four examined species.

226   The second and third tests involved counterfactual simulations of the four species. Both

227 simulations involved stabilizing the demographic rates of an individual size class (*i.e.*, j)

228 toward their arithmetic mean across a simulated timeseries of 1,000 timesteps. This

229 stabilization approach tests a key assumption of measures of demographic buffering: whether

230 the degree to which a stage class is demographically buffered implicates the degree to which

231 the whole population would benefit from the stabilization of demographic rates in said stage

232 class. If a measure of demographic buffering is effective, we predict a positive relationship

233 between the degree of stage specific demographic buffering and the degree to which the

234 population benefits from the stabilization of demographic rates in each stage class along the

235 life cycle of the species.

236   To test H2, that there is a strong negative relationship between the degree of buffering

237 associated with an individual stage along an ontogeny and the improvement in population

238 growth associated with the stabilization of demographic rates associated with said stage (*i.e.*,

239 $\Delta\lambda_s$), we used a counterfactual approach. Specifically, we stabilized the demographic rates of

240 each size class one at a time, whilst leaving the demographic rates of all other stages to vary

241 through time. After running 1,000 simulations of the stabilized population timeseries, the mean

242 stochastic population growth rate of the *stabilized* population was calculated. The difference

243 between the stabilized stochastic population growth rate and the stochastic population growth

244 rate of the non-stabilized population timeseries was calculated (*i.e.*, $\Delta\lambda_s$). Subsequently,

245 measures of $\Delta\lambda_s$ were regressed against each measure of stage-specific demographic buffering

246   (*i.e.*, ρ, V_s, $V_s + V_c$ and $\sum E_{a_{ij}}^{\sigma^2}$). The degree to which $\Delta\lambda_s$ and the measures of stage-specific

247   demographic buffering negatively covary corresponds to the efficacy of the individual

248   measures of demographic buffering – *i.e.*, stabilizing demographic rates in the least buffered

249   stages producing greater $\Delta\lambda_s$ values than more buffered stages. Negative covariances were

250   assessed using Spearman's ρ correlations with significance attributed to $p < 0.05$.

251   To test H3, that the stabilization of demographic rates informed by size-class specific

252   demographic buffering distributions would yield a significantly higher $\Delta\lambda_s$ than a random

253   stabilization of demographic rates, we used another counterfactual approach. Specifically, we

254   stabilized the demographic rates relative to their measures of stage-specific demographic

255   buffering. In other words, if a stage class (*j*) were the least demographically buffered for a

256   specific measure of demographic buffering (*e.g.*, $\sum E_{a_{ij}}^{\sigma^2}$), that stage class would be stabilized

257   to its arithmetic mean. However, if a stage class were the most demographically buffered, the

258   timeseries would resemble the non-stabilized population timeseries. For intermediate levels of

259   demographic buffering, the population's timeseries of demographic rates was set to the

260   weighted average of the stabilized and non-stabilized population timeseries, relative to the

261   percentile the stage is demographically buffered (for more details, see Supplementary

262   Methods). To test for efficacy, we used a permutation approach. Specifically, we simulated

263   10,000 random distributions of demographic buffering and stabilized the timeseries of

264   demographic rates relative to these random distributions. This resulted in a null distribution of

265   how an ineffective measure of demographic buffering may stabilize the system. To test whether

266   the measures of demographic buffering are effective, we identified the 95th percentile within

267   the null distribution and attributed efficacy to any measure that was consistently greater than

268   the 95th percentile across all four species.

269

RESULTS

<u>Test 1: Identifying differences in the measures of demographic buffering across ontogeny</u>

In the first test, we aimed to identify whether the four measures of demographic buffering offer similar or distinct inferences across the four examined species. For this, we analysed the correlation structure of each measure of demographic buffering structured across ontogeny and found heterogeneity across the four species, thus supporting of H1 (Fig. 1). These differences are demonstrated by the differences in correlation patterns across the four species. Interestingly, the only pairwise combination of demographic buffering measures that offered a highly stereotyped correlation structure was V_s and $V_s + V_c$. These results are also mirrored with a principal component analysis of the measures of demographic buffering across the four species (Supplementary Fig. 1).

286

287
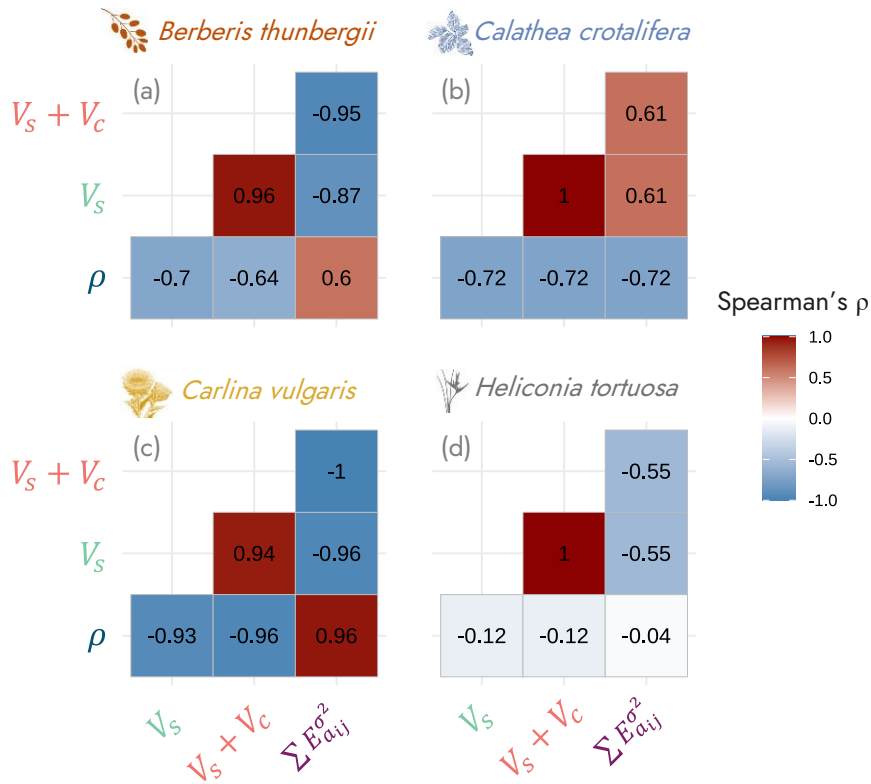
Figure 1: Heterogeneity in the measures of demographic buffering. Here, we show the correlation structure of four measures of demographic buffering structured across ontogeny for all four plant species. The four measures are: Spearman's ρ coefficient correlating elasticities and CV values associated with individual demographic rates, V_s which quantifies the impact of demographic rate variance on population growth using Tuljapurkar's approximation, $V_s + V_c$ which quantifies the impact of demographic rate variance and covariances on population growth using Tuljapurkar's approximation and the summed stochastic elasticities of variance ($\sum E_{a_{ij}}^{\sigma^2}$). The numbers in the centre of the cells represent the Spearman's ρ coefficient associated with pairwise combinations of the demographic buffering measures. Redder (bluer) tones correspond to more positive (negative) correlations.

298

299

300

301

302

Test 2: Testing for efficacy by stabilizing demographic rates across individual stages

304   In the second test, we quantified the efficacy in each measure of demographic buffering.

305   Specifically, we hypothesized (H2) that individual simulations of each species, where the

306   demographic rates of each stage were stabilized (*i.e.*, re-parameterized to be constant through

307   time) one stage at a time, would lead to a negative relationship between the degree of buffering

308   associated with a specific stage and $\Delta\lambda_s$. The rationale for this hypothesis is the stabilization

309   of demographic rates in individual stages should have a larger positive effect in the least

310   buffered stages than in more buffered stages. Of the four different methods for calculating

311   demographic buffering, only $\sum E_{a_{ij}}^{\sigma^2}$ generated negative relationships between degree of

312   buffering and $\Delta\lambda_s$ across the four species (Spearman's ρ, $p < 0.05$; Fig. 2). The other metrics

313   (*i.e.*, ρ, V_s and $V_s + V_c$) only generated negative relationships between degree of buffering and

314    $\Delta\lambda_s$ in *Berberis thunbergii* and *Carlina vulgaris* (Spearman's ρ, $p < 0.05$; Fig. 2). In turn, the

315   second test indicates $\sum E_{a_{ij}}^{\sigma^2}$ is the only measure of demographic buffering that is predictably

316   effective across all four examined species.

317

318

319

320

321

322

323

324

325

326
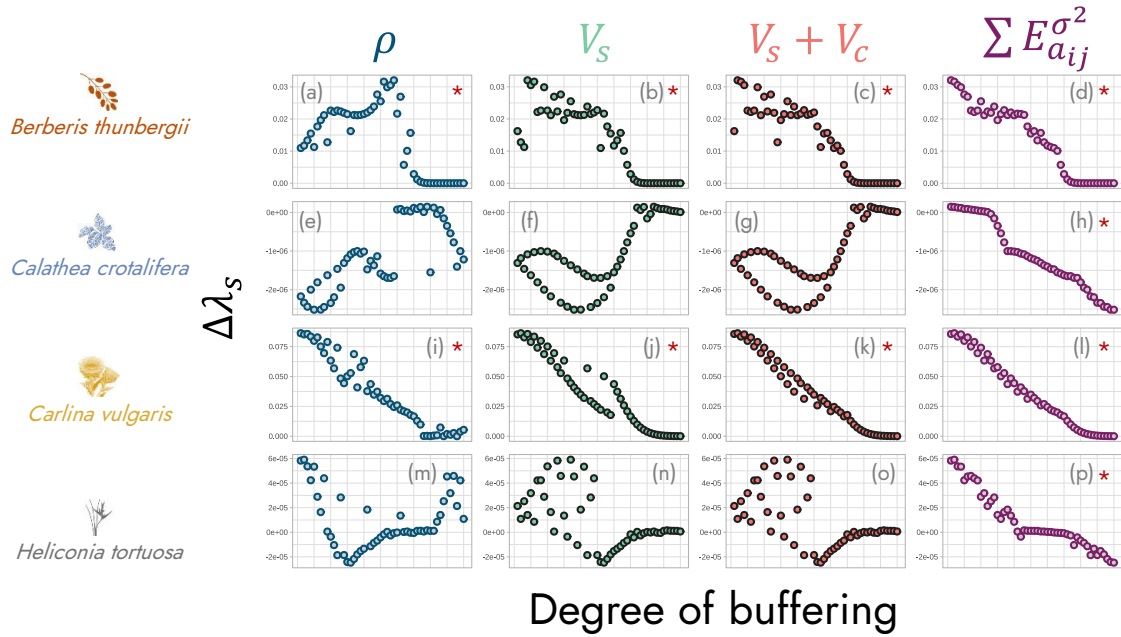
Figure 2: Stabilization of demographic rates across the life cycle of four examined species identifies $\sum E_{a_{ij}}^{\sigma^2}$ as an effective measure of demographic buffering. Here, the results from the simulations where demographic rates were stabilized for stages one at a time are shown – rows indicate species whilst columns represent the different measures of demographic buffering. The four measures are: Spearman's ρ coefficient correlating elasticities and CV values associated with individual demographic rates, V_s which quantifies the impact of demographic rate variance on population growth using Tuljapurkar's approximation, $V_s + V_c$ which quantifies the impact of demographic rate variance and covariances on population growth using Tuljapurkar's approximation and the summed stochastic elasticities of variance $(\sum E_{a_{ij}}^{\sigma^2})$. The x-axis of each graph represents the degree of buffering from least buffering (on the left) to the most buffered (on the right). The y-axis represents the change in stochastic population growth rate ($\Delta\lambda_s$) due to the stabilization of demographic rates in the associated stage. Significant negative relationships (assessed by Spearman's ρ, $p < 0.05$) are shown with red asterisks.

341

342

343

344

345

346 <u>Test 3: Testing for efficacy by stabilizing demographic rates weighted by the distribution of</u>

347 <u>demographic buffering across ontogeny</u>

348 In the third test, we quantified the efficacy in each measure of demographic buffering.

349 Specifically, we test (H3) whether stabilizing demographic rates relative to the distribution of

350 demographic buffering across ontogeny outperforms stabilization measures that were not

351 informed by demographic buffering measures. From these simulations, we found $\sum E_{a_{ij}}^{\sigma^2}$ is the

352 only measure of demographic buffering that performs better than chance in improving the

353 population's stochastic growth rate ($\Delta\lambda_s$) (Fig. 3). This is shown by all $\Delta\lambda_s$ values associated

354 with $\sum E_{a_{ij}}^{\sigma^2}$ being greater than the 95th percentile of the simulated null distribution.

355

356

357

358

359

360

361

362

363

364

365

$\Delta\lambda_s$
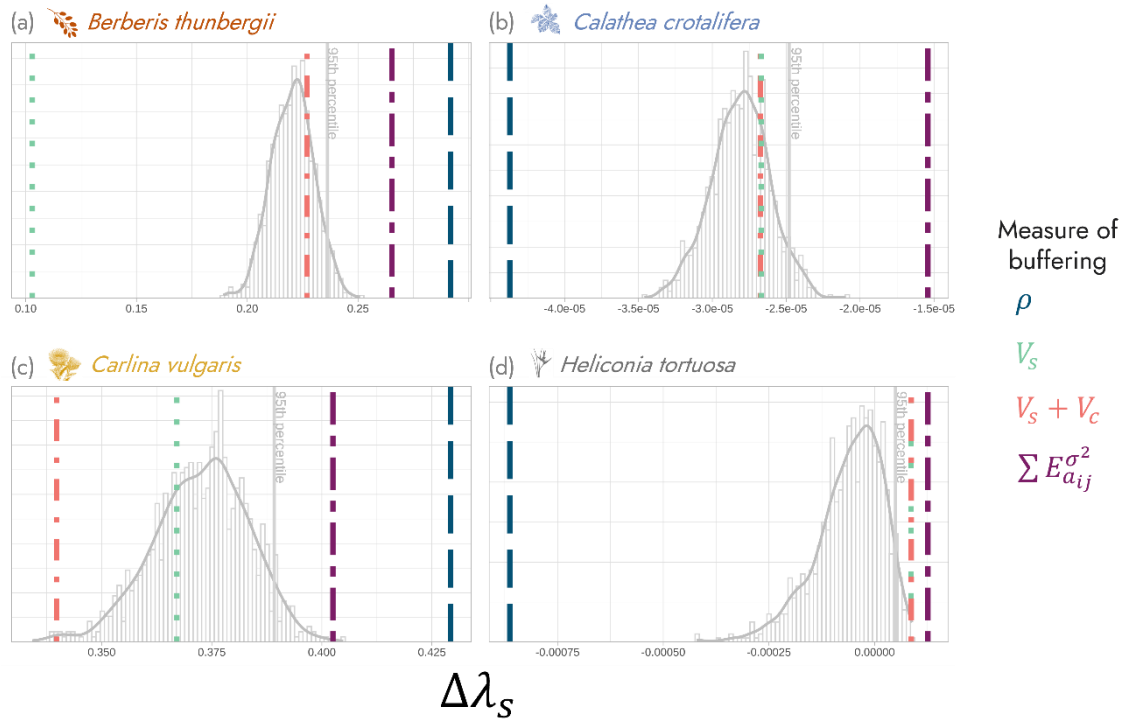
Figure 3: Stabilization of demographic rates weighted by the distribution of buffering across ontogeny indicates $\sum E_{a_{ij}}^{\sigma^2}$ is an effective measure of demographic buffering. Here, the results for simulations where demographic rate variances are stabilized relative to each measure of demographic buffering are shown. The four measures are: Spearman's ρ coefficient correlating elasticities and CV values associated with individual demographic rates, V_s which quantifies the impact of demographic rate variance on population growth using Tuljapurkar's approximation, $V_s + V_c$ which quantifies the impact of demographic rate variance and covariances on population growth using Tuljapurkar's approximation and the summed stochastic elasticities of variance ($\sum E_{a_{ij}}^{\sigma^2}$). The grey histograms represent the null distributions (*i.e.*, populations stabilized by a random buffering distribution), and the grey vertical line represents the 95th percentile of the null distribution. In this test, efficacy is attributed to a measure of demographic buffering that is consistently greater than the 95th percentile across all four species (*i.e.*, $\sum E_{a_{ij}}^{\sigma^2}$). The patterned vertical lines represent values of $\Delta\lambda_s$ for populations stabilized by the individual measures of demographic buffering.

DISCUSSION

In this study, we aimed to test for efficacy across four measures of demographic buffering. To test for efficacy, we used four IPMs associated with plants with different life histories [*i.e.*, one herbaceous perennial (*Berberis thunbergii*, Merow et al., 2017), two tropical perennials (*Calathea crotalifera* and *Heliconia tortuosa*, (Westerband & Horvitz, 2017)) and a biennial plant (*Carlina vulgaris*, Rees & Ellner, 2009)]. Collectively, our findings identify the summation of stochastic elasticities of variance ($\sum E_{a_{ij}}^{\sigma^2}$) as the most effective measure of demographic buffering over three other metrics: Spearman's ρ coefficient correlating elasticities and CV values associated with individual demographic rates, V_s which quantifies the impact of demographic rate variance on population growth using Tuljapurkar's approximation and $V_s + V_c$ which quantifies the impact of demographic rate variance and covariances on population growth using Tuljapurkar's approximation. This efficacy is supported by three independent tests. In test 1, the stage-based measures of demographic buffering were shown to have different correlation structures across the four species (Fig. 1, Supplementary Fig. 1). This disparity of results indicates the four measures are not measuring demographic buffering in the same manner. In tests 2 and 3, the measures differed in their efficacy to infer a population's response to simulations of reduced demographic rate variance (Figs. 2,3). Specifically, only $\sum E_{a_{ij}}^{\sigma^2}$ was consistently effective across all four species in both tests 2 and 3.

Our findings have broad implications for past and future studies of demographic buffering. Previous studies have primarily focused on the correlation method (*i.e.*, ρ) for studies of individual populations (Hilde et al., 2020) or comparative approaches (McDonald et al., 2017) with few studies using $\sum E_{a_{ij}}^{\sigma^2}$ (but see Morris et al., 2008). This is problematic as tests 2 and 3 show stage-based conservation measures based on the correlation approach to be

18

410   ineffective – especially in contrast to $\sum E_{a_{ij}}^{\sigma^2}$. While previous work has shown the correlation-

411   based approach to (1) have a phylogenetic signal across plant species (McDonald et al., 2017),

412   (2) signal buffering *versus* labile strategies in variable environments (Li & Ramula, 2015) and

413   (3) potentially be an axis of life history variation (Salguero-Gómez, 2021), we suggest these

414   inferences might not extend to structured conservation measures of populations in variable

415   environments. To fully connect our findings to previous literature, future work should focus on

416   reanalysing results from broad comparative analyses (McDonald et al., 2017; Morris et al.,

417   2008) using multiple measures – especially $\sum E_{a_{ij}}^{\sigma^2}$ – to test previous findings.

418   Whilst these findings offer new insights to the efficacy of demographic buffering

419   measures, inferences drawn from these findings have important limitations. First, the degree to

420   which the generality of these findings are constrained to certain life histories remains unknown.

421   Whilst here we used species with different life history strategies (*i.e.*, one herbaceous perennial,

422   two tropical perennials and one biennial), the extent to which these findings may apply to more

423   unique life histories (*e.g.*, eusocial insects, migratory megafauna or semelparous fish) is

424   unknown and open to future research. Second, our results indicate that the measures of

425   demographic buffering are in fact different and should, therefore, be treated as such. This is

426   not to say that only $\sum E_{a_{ij}}^{\sigma^2}$ has a place in the buffering literature. For example, important

427   research can – and has – been directed at other terms from Tuljapurkar's approximation to infer

428   population responses to changes in environmental stochasticity (Compagnoni et al., 2016,

429   2021; Evers et al., 2023; Paniw et al., 2018). And third, the test for efficacy is stage specific,

430   because structured populations often incur stage structured perturbations. For example, hunting

431   and extreme events can perturb demographic processes unevenly across a life cycle (Darimont

432   & Child, 2014; von Takach Dukai et al., 2018). However, whilst our approach is more in

433   keeping with the ecological dynamics of structured populations, the theory around

434   demographic buffering is agnostic of stage specific perturbations (Hilde et al., 2020; Morris et

435   al., 2008; Pfister, 1998; but see Gaillard et al., 1998). Therefore, the inefficacy of ρ, V_s and

436      $V_s + V_c$ can only be attributed to stage explicit inferences of demographic buffering, not

437   interpretations at the level of the whole population (Rodríguez-Caro et al., 2021) or across

438   species (Pfister, 1998).

439   In the future, demographic buffering could be connected to two previously disparate

440   corners of ecology and evolution. First, variance in demographic rates is not the sole driver of

441   population extinction and persistence in variable environments (Capdevila et al., 2020;

442   Hastings et al., 2018; McDonald et al., 2016). Indeed, transient dynamics, temporary

443   fluctuations in populations that decay over time due to progressive shifts toward a stable

444   age/stage/size structure, are also at play (Stott et al., 2011, 2012; Tuljapurkar et al., 2023).

445   Recent research has shown the transient portfolio of populations in response to disturbance to

446   have broad impacts on population trajectories (Capdevila et al., 2020; Ezard et al., 2010;

447   Jackson et al., 2019; McDonald et al., 2016; White et al., 2013). Furthermore, the transient

448   portfolio can be the mechanism by which the population is able to persist (Hansen et al., 2019)

449   and be a key contributor to the variance of population growth rate overtime (Jelbert et al., 2019;

450   McDonald et al., 2016). Unfortunately, previous papers focusing on demographic buffering

451   have been agnostic to the transient dynamics in their populations of interest – thereby making

452   this a key area for future work. Second, the link between demographic buffering and life history

453   evolution is incomplete. The components that build all measures of demographic buffering are

454   in some way connected to the sensitivies or elasticities of population growth rate (λ) in

455   response to changes in demographic rates. These sensitivities and elasticities are often used to

456   infer ecological processes (*e.g.*, demographic buffering) but also selection gradients (Brodie et

457   al., 1995; Caswell, 1978). Whilst previous work has implicated demographic buffering as a life

458   history strategy (Jongejans et al., 2010; Koons et al., 2009; Rodríguez-Caro et al., 2021), there

459 is no evidence for selection acting on any measure of demographic buffering in a natural

460 population. In turn, future work must be aimed at filling this gap in knowledge.

461   In conclusion, we have shown: (1) the efficacy of $\sum E_{a_{ij}}^{\sigma^2}$ as a measure of demographic

462 buffering, (2) how different measures of demographic buffering report different values for the

463 same populations of interest and (3) the utility of counterfactual simulations to test for efficacy

464 in metrics of interest. This work supports previous uses of $\sum E_{a_{ij}}^{\sigma^2}$ (Gascoigne, Kajin,

465 Tuljapurkar, et al., 2023; Morris et al., 2008; Santos et al., 2023; Westerband & Horvitz, 2017)

466 and opens new avenues of research to both confirm previous findings and extend ideas

467 surrounding demographic buffering to other areas of ecology and evolution.

468

477

478

479

480

REFERENCES

Bathiany, S., Dakos, V., Scheffer, M., & Lenton, T. M. (2018). Climate models predict increasing temperature variability in poor countries. *Science Advances*, *4*(5), 1–11. https://doi.org/10.1126/sciadv.aar5809

Brodie, E. D., Moore, A., & Janzen, F. (1995). Visualizing and quantifying natural selection. *Trends in Ecology and Evolution*, *10*(8), 313–318.

Capdevila, P., Stott, I., Beger, M., & Salguero-Gómez, R. (2020). Towards a Comparative Framework of Demographic Resilience. *Trends in Ecology and Evolution*, *35*(9), 776–786. https://doi.org/10.1016/j.tree.2020.05.001

Caswell, H. (1978). A general formula for the sensitivity of population growth rate to changes in life history parameters. *Theoretical Population Biology*, *14*, 215–230.

Caswell, H. (2001). *Matrix population models: Construction, analysis, and interpretation* (2nd editio). Sinauer.

Colchero, F., Eckardt, W., & Stoinski, T. (2021). Evidence of demographic buffering in an endangered great ape: social buffering on immature survival and the role of refined sex-age-classes on population growth rate. *Journal of Animal Ecology*, *90*(7), 1365–2656. https://doi.org/10.1111/1365-2656.13486

Compagnoni, A., Bibian, A. J., Ochocki, B. M., Rogers, H. S., Schultz, E. L., Sneck, M. E., Elderd, B. D., Iler, A. M., Inouye, D. W., Jacquemyn, H., & Miller, T. E. X. (2016). The effect of demographic correlations on the stochastic population dynamics of perennial plants. *Ecological Monographs*, *86*(4), 480–494. https://doi.org/10.1002/ecm.1228

Compagnoni, A., Levin, S., Childs, D. Z., Harpole, S., Paniw, M., Römer, G., Burns, J. H., Che-Castaldo, J., Rüger, N., Kunstler, G., Bennett, J. M., Archer, C. R., Jones, O. R., Salguero-Gómez, R., & Knight, T. M. (2021). Herbaceous perennial plants with short generation time have stronger responses to climate anomalies than those with longer generation time. *Nature Communications*, *12*(1), 1–8. https://doi.org/10.1038/s41467-021-21977-9

Darimont, C. T., & Child, K. R. (2014). What enables size-selective trophy hunting of wildlife? *PLoS ONE*, *9*(8). https://doi.org/10.1371/journal.pone.0103487

De Kroon, H., Plaisier, A., Van Groenendael, J., & Caswell, H. (1986). *Elasticity: The Relative Contribution of Demographic Parameters to Population Growth Rate* (Vol. 67, Issue 5).

Easterling, M. R., Ellner, S. P., & Dixon, P. M. (2000). Size-specific sensitivity: Applying a new structured population model. *Ecology*, *81*(3), 694–708.

Ellner, S. P., Childs, D. Z., & Rees, M. (2016). *Data-driven Modelling of Structured Populations* (Issue 2000).

Evers, S. M., Knight, T. M., & Compagnoni, A. (2023). The inclusion of immediate and lagged climate responses amplifies the effect of climate autocorrelation on long-term

growth rate of populations. *Journal of Ecology*, 1–12. https://doi.org/10.1111/1365-2745.14155

Ezard, T. H. G., Bullock, J. M., Dalgleish, H. J., Millon, A., Pelletier, F., Ozgul, A., & Koons, D. N. (2010). Matrix models for a changeable world: The importance of transient dynamics in population management. *Journal of Applied Ecology*, *47*(3), 515–523. https://doi.org/10.1111/j.1365-2664.2010.01801.x

Gaillard, J.-M., Festa-Bianchet, M., & Yoccoz, N. G. (1998). Population dynamics of large herbivores: variable recruitment with constant adult survival. *Trends in Ecology & Evolution*, *13*(2), 249–251.

Gascoigne, S. J. L., Kajin, M., & Salguero-Gómez, R. (2023). Criteria for buffering in ecological modeling. *Trends in Ecology & Evolution*. https://doi.org/10.1016/j.tree.2023.11.006

Gascoigne, S. J. L., Kajin, M., Tuljapurkar, S., Silva Santos, G., Steiner, U. K., Vinton, A. C., Jaggi, H., Sepil, I., & Salguero-Gómez, R. (2023). Structured demographic buffering: A framework to explore the environment drivers and demographic mechanisms underlying demographic buffering. *BioRxiv*. https://doi.org/10.1101/2023.07.20.549848

Hansen, B. B., Gamelon, M., Albon, S. D., Lee, A. M., Stien, A., Irvine, R. J., Sæther, B. E., Loe, L. E., Ropstad, E., Veiberg, V., & Grøtan, V. (2019). More frequent extreme climate events stabilize reindeer population dynamics. *Nature Communications*, *10*, 1616. https://doi.org/10.1038/s41467-019-09332-5

Haridas, C. V., & Tuljapurkar, S. (2005). Elasticities in variable environments: Properties and implications. *American Naturalist*, *166*(4), 481–495. https://doi.org/10.1086/444444

Hastings, A., Abbott, K. C., Cuddington, K., Francis, T., Gellner, G., Lai, Y. C., Morozov, A., Petrovskii, S., Scranton, K., & Zeeman, M. Lou. (2018). Transient phenomena in ecology. *Science*, *361*(6406). https://doi.org/10.1126/science.aat6412

Hilde, C. H., Gamelon, M., Sæther, B. E., Gaillard, J. M., Yoccoz, N. G., & Pélabon, C. (2020). The Demographic Buffering Hypothesis: Evidence and Challenges. *Trends in Ecology and Evolution*, *35*(6), 523–538. https://doi.org/10.1016/j.tree.2020.02.004

Jackson, J., Childs, D. Z., Mar, K. U., Htut, W., & Lummaa, V. (2019). Long-term trends in wild-capture and population dynamics point to an uncertain future for captive elephants. *Proceedings. Biological Sciences*, *286*(1899), 20182810. https://doi.org/10.1098/rspb.2018.2810

Jelbert, K., Buss, D., McDonald, J., Townley, S., Franco, M., Stott, I., Jones, O., Salguero-Gómez, R., Buckley, Y., Knight, T., Silk, M., Sargent, F., Rolph, S., Wilson, P., & Hodgson, D. (2019). Demographic amplification is a predictor of invasiveness among plants. *Nature Communications*, *10*(1). https://doi.org/10.1038/s41467-019-13556-w

Jongejans, E., de Kroon, H., Tuljapurkar, S., & Shea, K. (2010). Plant populations track rather than buffer climate fluctuations. *Ecology Letters*, *13*(6), 736–743. https://doi.org/10.1111/j.1461-0248.2010.01470.x

Koons, D. N., Pavard, S., Baudisch, A., & Metcalf, C. J. E. (2009). Is life-history buffering or lability adaptive in stochastic environments? *Oikos*, *118*(7), 972–980. https://doi.org/10.1111/j.1600-0706.2009.16399.x

Levin, S. C., Evers, S., Potter, T., Guerrero, M. P., Childs, D. Z., Compagnoni, A., Knight, T. M., & Salguero-Gómez, R. (2022). Rpadrino: An R package to access and use PADRINO , an open access database of Integral Projection Models . *Methods in Ecology and Evolution*, *2022*(May), 1–7. https://doi.org/10.1111/2041-210x.13910

Li, S. L., & Ramula, S. (2015). Demographic strategies of plant invaders in temporally varying environments. *Population Ecology*, *57*(2), 373–380. https://doi.org/10.1007/s10144-015-0479-0

Maldonado-Chaparro, A. A., Blumstein, D. T., Armitage, K. B., & Childs, D. Z. (2018). Transient LTRE analysis reveals the demographic and trait-mediated processes that buffer population growth. *Ecology Letters*, *21*(11), 1693–1703. https://doi.org/10.1111/ele.13148

Masson-Delmotte, V., Zhai, P., Pirani, A., Connors, S. L., Péan, C., Berger, S., Caud, N., Chen, Y., Goldfarb, L., Gomis, M. I., Huang, M., Leitzell, K., Lonnoy, E., Matthews, J. B. R., Maycock, T. K., Waterfield, T., Yelekçi, O., Yu, R., & Zhou, B. (2021). IPCC: Climate Change 2021: The Physical Science Basis. *Cambridge University Press. In Press.*

May, R. M. (1973). Stability in randomly fluctuating versus deterministic environments. *The American Naturalist*, *107*(957), 621–650. https://doi.org/10.1086/282863

McDonald, J. L., Franco, M., Townley, S., Ezard, T. H. G., Jelbert, K., & Hodgson, D. J. (2017). Divergent demographic strategies of plants in variable environments. *Nature Ecology and Evolution*, *1*(2), 0029. https://doi.org/10.1038/s41559-016-0029

McDonald, J. L., Stott, I., Townley, S., & Hodgson, D. J. (2016). Transients drive the demographic dynamics of plant populations in variable environments. *Journal of Ecology*, *104*(2), 306–314. https://doi.org/10.1111/1365-2745.12528

Merow, C., Bois, S. T., Allen, J. M., Xie, Y., & Silander, J. A. (2017). Climate change both facilitates and inhibits invasive plant ranges in New England. *Proceedings of the National Academy of Sciences of the United States of America*, *114*(16), E3276–E3284. https://doi.org/10.1073/pnas.1609633114

Morris, W. F., & Doak, D. F. (2004). Buffering of Life Histories against Environmental Stochasticity: Accounting for a Spurious Correlation between the Variabilities of Vital Rates and Their Contributions to Fitness. *American Naturalist*, *163*(4), 579–590. https://doi.org/10.1086/382550

Morris, W. F., Pfister, C. A., Tuljapurkar, S., Haridas, C. V., Boggs, C. L., Boyce, M. S., Bruna, E. M., Church, D. R., Coulson, T., Doak, D. F., Forsyth, S., Gaillard, J. M., Horvitz, C. C., Kalisz, S., Kendall, B. E., Knight, T. M., Lee, C. T., & Menges, E. S. (2008). Longevity can buffer plant and animal populations against changing climatic variability. *Ecology*, *89*(1), 19–25. http://www.esajournals.org/doi/pdf/10.1890/07-0774.1

Paniw, M., Ozgul, A., & Salguero-Gómez, R. (2018). Interactive life-history traits predict sensitivity of plants and animals to temporal autocorrelation. *Ecology Letters*, *21*(2), 275–286. https://doi.org/10.1111/ele.12892

Pfister, C. A. (1998). Patterns of variance in stage-structured populations: Evolutionary predictions and ecological implications. *Proceedings of the National Academy of Sciences of the United States of America*, *95*(1), 213–218. https://doi.org/10.1073/pnas.95.1.213

Raventós, J., Mújica, E., González, E., Bonet, A., & Ortega-Larrocea, M. P. (2021). The effects of hurricanes on the stochastic population growth of the endemic epiphytic orchid Broughtonia cubensis living in Cuba. *Population Ecology*, *63*(4), 302–312. https://doi.org/10.1002/1438-390X.12098

Rees, M., & Ellner, S. P. (2009). Integral projection models for populations in temporally varying environments. *Ecological Monographs*, *79*(4), 575–594. https://doi.org/10.1890/08-1474.1

Rodríguez-Caro, R. C., Capdevila, P., Graciá, E., Barbosa, J. M., Giménez, A., & Salguero-Gómez, R. (2021). The limits of demographic buffering in coping with environmental variation. *Oikos*, *130*(8), 1346–1358. https://doi.org/10.1111/oik.08343

Salguero-Gómez, R. (2021). Commentary on the life history special issue: The fast-slow continuum is not the end-game of life history evolution, human or otherwise. *Evolution and Human Behavior*, *42*(3), 281–283. https://doi.org/10.1016/j.evolhumbehav.2021.03.005

Santos, G. S., Gascoigne, S. J. L., Dias, A. T. C., Kajin, M., & Salguero-Gómez, R. (2023). A unified framework to identify demographic buffering in natural populations. *BioRxiv*, 1–31.

Stott, I., Hodgson, D. J., & Townley, S. (2012). Beyond sensitivity: Nonlinear perturbation analysis of transient dynamics. *Methods in Ecology and Evolution*, *3*(4), 673–684. https://doi.org/10.1111/j.2041-210X.2012.00199.x

Stott, I., Townley, S., & Hodgson, D. J. (2011). A framework for studying transient dynamics of population projection matrix models. *Ecology Letters*, *14*(9), 959–970. https://doi.org/10.1111/j.1461-0248.2011.01659.x

Sutherland, W. J., Freckleton, R. P., Godfray, H. C. J., Beissinger, S. R., Benton, T., Cameron, D. D., Carmel, Y., Coomes, D. A., Coulson, T., Emmerson, M. C., Hails, R. S., Hays, G. C., Hodgson, D. J., Hutchings, M. J., Johnson, D., Jones, J. P. G., Keeling, M. J., Kokko, H., Kunin, W. E., … Wiegand, T. (2013). Identification of 100 fundamental ecological questions. *Journal of Ecology*, *101*(1), 58–67. https://doi.org/10.1111/1365-2745.12025

Tuljapurkar, S. (1982). Population dynamics in variable environments. III. Evolutionary dynamics of r-selection. *Theoretical Population Biology*, *21*(1), 141–165. https://doi.org/10.1016/0040-5809(82)90010-7

Tuljapurkar, S. (1989). An uncertain life: Demography in random environments. *Theoretical Population Biology*, *35*(3), 227–294. https://doi.org/10.1016/0040-5809(89)90001-4

640   Tuljapurkar, S. (1990). *Population dynamics in variable environments*. Springer-Verlag.

641   Tuljapurkar, S., Horvitz, C. C., & Pascarella, J. B. (2003). The Many Growth Rates and
642   Elasticities of Populations in Random Environments. *American Naturalist*, *162*(4).

643   Tuljapurkar, S., Jaggi, H., Gascoigne, S. J. L., Zuo, W., Kajin, M., & Salguero-Gómez, R.
644   (2023). From disturbances to nonlinear fitness and back. *BioRxiv*.
645   https://doi.org/10.1101/2023.10.20.563360

646   von Takach Dukai, B., Lindenmayer, D. B., & Banks, S. C. (2018). Environmental influences
647   on growth and reproductive maturation of a keystone forest tree: Implications for
648   obligate seeder susceptibility to frequent fire. *Forest Ecology and Management*, *411*,
649   108–119. https://doi.org/10.1016/j.foreco.2018.01.014

650   Westerband, A. C., & Horvitz, C. C. (2017). Photosynthetic rates influence the population
651   dynamics of understory herbs in stochastic light environments. *Ecology*, *98*(2), 370–381.
652   https://doi.org/10.1002/ecy.1664

653   White, J. W., Botsford, L. W., Hastings, A., Baskett, M. L., Kaplan, D. M., & Barnett, L. A.
654   K. (2013). Transient responses of fished populations to marine reserve establishment.
655   *Conservation Letters*, *6*(3), 180–191. https://doi.org/10.1111/j.1755-263X.2012.00295.x

656

657

658

659

660

661

662

663

664

665

666

667

668

669

670

671

672

Testing for efficacy in four measures of demographic buffering

Samuel J L Gascoigne[1,*], Maja Kajin[1,2], Irem Sepil[1], Roberto Salguero-Gómez[1,3]

Supplementary online materials

[1] Department of Biology, South Parks Road, University of Oxford, Oxford, United Kingdom

[2] Department of Biology, Biotechnical Faculty, University of Ljubljana, Večna pot 111, 1000 Ljubljana, Slovenia

[3] National Laboratory for Grassland & Agro-ecosystems, Lanzhou University, China

* Correspondence: samuel.gascoigne@abdn.ac.uk

704   **SUPPLEMENTARY METHODS**

705   To perform the counterfactual simulations used in test 3, we stabilized the demographic rates

706   associated with each stage (*i.e.*, where the demographic rate is a_{ij} and the focal stage is j)

707   relative to the degree of buffering associated with each stage (DB_j). Note, here DB_j represents

708   the degree of buffering associated with each measure of demographic buffering (*i.e.*, $\rho, V_s, V_s +$

709   V_c and $\sum E_{a_{ij}}^{\sigma^2}$) individually. The method by which we stabilized demographic rates is as

710   follows.

711   First, we calculated the distribution of demographic buffering across ontogeny and

712   scaled the values between 0 and 1. The scaled values (β_j) were calculated as:

713           $$\beta_j = \frac{DB_j - \min(DB_j)}{\max(DB_j) - \min(DB_j)}.$$

714   This scaling means that a β_j value of 0 is the least buffered stage whilst a β_j value of 1 is the

715   most buffered stage.[2]

716   Second, we used the original time series of demographic rates ($a_{ij,t}$) and the β_j

717   distribution to generate a new series of demographic rates ($a_{ij,t}^*$) that are stabilized toward the

718   mean demographic rate ($\overline{a_{ij}}$) proportional to β_j:

719           $$a_{ij,t}^* = \beta_j(a_{ij,t}) + (1 - \beta_j)(\overline{a_{ij}}).$$

720   In other words, if a stage class (j) were the least demographically buffered for a specific

721   measure of demographic buffering ($\sum E_{a_{ij}}^{\sigma^2}$), that stage class would be stabilized to its

722   arithmetic mean. However, if a stage class were the most demographically buffered, the time

723   series would resemble the non-stabilized population time series.

724

725

726

---

[2] It is worth noting that the relationship between the valued inferred from the measure of demographic buffering and degree of buffering varies across each measure. Specifically, ρ, V_s and $V_s + V_c$ have a negative relationship with degree of demographic buffering. However, $\sum E_{a_{ij}}^{\sigma^2}$ has a positive relationship with demographic buffering. In turn, all values were transformed to be both positive (as ρ and $\sum E_{a_{ij}}^{\sigma^2}$ can have negative values) and have a positive relationship with the inferred degree of demographic buffering.

728
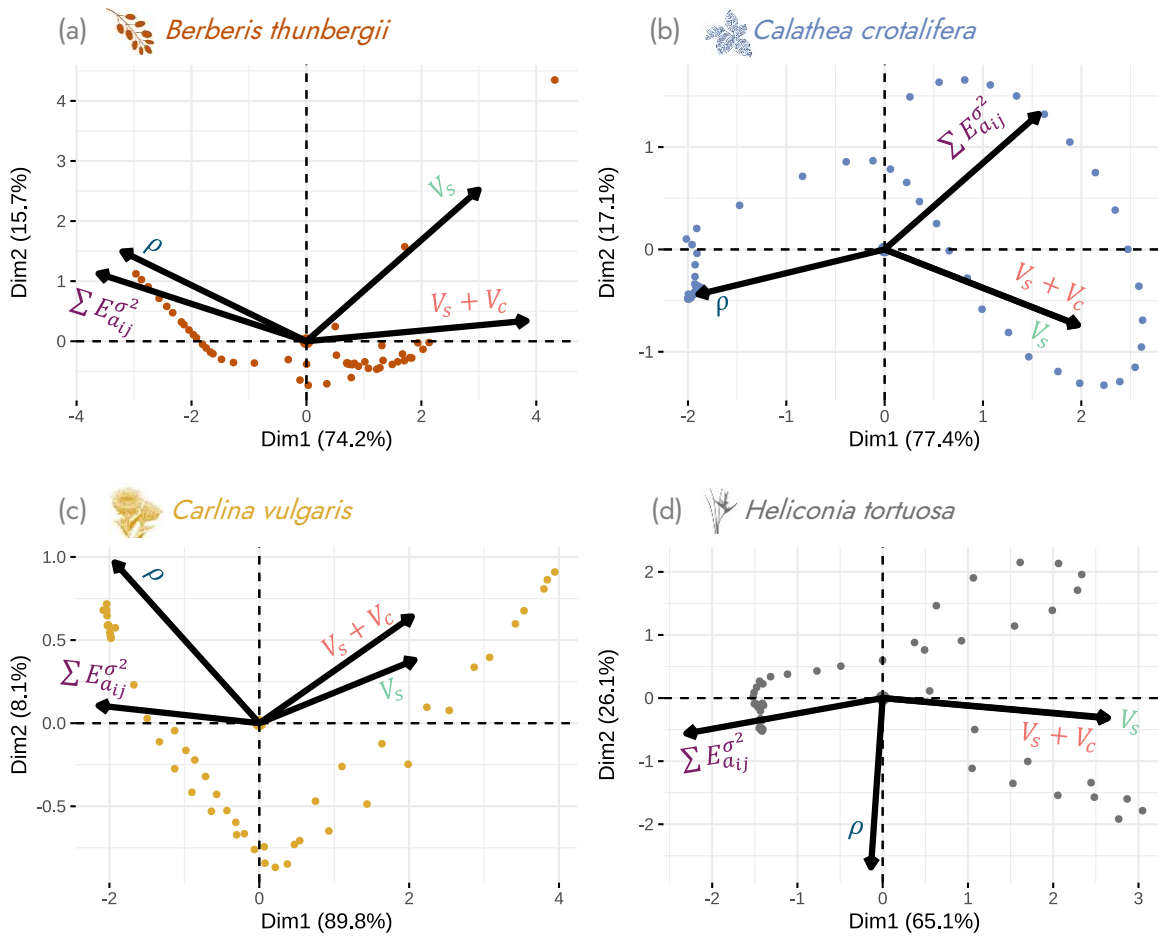
729

730

731 **Supplementary Figure 1: Heterogeneity in the measures of demographic buffering.** Here
732 we show the covariance structure, via a principal component analysis (PCA), of four different
733 measures of demographic buffering, structured across ontogeny, for four species of plants. The
734 four measures are: Spearman's ρ coefficient correlating elasticities and CV values associated
735 with individual demographic rates, V_s which quantifies the impact of demographic rate variance
736 on population growth using Tuljapurkar's approximation, $V_s + V_c$ which quantifies the impact
737 of demographic rate variance and covariances on population growth using Tuljapurkar's
738 approximation and the summed stochastic elasticities of variance ($\sum E_{a_{ij}}^{\sigma^2}$). Prior to running the
739 PCA, all values were scaled and centred. The points represent buffering values associated with
740 individual stages across the life history of each species. The arrows represent the covariance
741 structure of each measure of demographic buffering. It is worth noting that the arrows for V_s
742 and $V_s + V_c$ are almost perfectly overlapping in the plots for *Calathea crotalifera* and *Heliconia*
743 *tortuosa*.

744

745

SUPPLEMENTARY TABLES

Supplementary Table 1: Formulas, regressions and parameters used to construct the IPMs for _Berberis thunbergii_.

Construction		Model	Parameter
Density-independent environmentally stochastic IPM		$n(z', t + 1) = \int_{\alpha}^{\omega} K(z', z, \psi_t) n(z, t) dz$	$\alpha = 2$ $\omega = 25$ $z = \log(\text{plant area})$
		$\psi_t = \{T_t, P_t, PAR_t, N_t, pH_t\}$	ψ = an array containing climate values
K-kernel		$K(z', z, \psi_t) = P(z', z, \psi_t) + F(z', z, \psi_t)$	
Sub-kernels	**P**-subkernel	$P(z', z, \psi_t) = s(z, \psi_t) * g(z', z, \psi_t)$	
	F-subkernel	$F(z', z, \psi_t) = f_s(z) * fl_p(z) * germ_p(\psi_t)$ $* sdl_s(z')$	
Demographic functions	Survival	$\text{logit}(s(z, \psi_t)) = s_i + s_z * z + s_T * T_t + s_P * P_t$ $+ s_{PAR} * PAR_t + s_N * N_t + s_{pH}$ $* pH_t$	$s_i = -11.8$ $s_z = 1.05$ $s_T = 1.11$ $s_P = 0.22$ $s_{PAR} = -0.52$ $s_N = -0.1$ $s_{pH} = 0.11$
	Growth	$g(z', z, \psi_t) = \text{dnorm}(z', g_\mu(z, \psi_t), g_{sd})$	$g_{sd} = 1.48$
		$g_\mu(z, \psi_t) = g_z * z + g_T * T_t + g_P * P_t + g_{PAR}$ $* PAR_t + g_N * N_t + g_{pH} * pH_t$	$g_z = 1.02$ $g_T = 0.65$ $g_P = 0.02$ $g_{PAR} = 0.59$ $g_N = -0.04$ $g_{pH} = 0.4$
	Reproduction	$f_s(z) = \exp(seed_i + seed_z * z)$	$seed_i = -23.01$ $seed_z = 1.32$
		$\text{logit}(fl_p(z)) = fl_i + fl_z * z$	$fl_i = -33.43$ $fl_z = 1.68$
		$\text{logit}(germ_p(\psi_t)) = germ_i + germ_T * T_t$ $+ germ_P * P_t + germ_{PAR}$ $* (PAR_t / 0.018) + germ_{pH}$ $* pH_t$	$germ_i = -11.8$ $germ_T = 0.51$ $germ_P = -0.02$ $germ_{PAR} = -0.02$ $germ_{pH} = 0.26$
		$sdl_s(z') = \text{dnorm}(z', sdl_\mu, sdl_{sd})$	$sdl_\mu = 10.23$ $sdl_{sd} = 1.581$
Environment values	Mean temperature in warmest month	$T \sim N(0, 1.5)$	
	Mean May precipitation	$P \sim N(0, 1.5)$	
	PAR	$PAR \sim N(0, 1.5)$	
	Soil Nitrogen	$N \sim N(0, 1.5)$	
	Soil pH	$pH \sim N(0, 1.5)$	

Supplementary Table 2: Formulas, regressions and parameters used to construct the
IPMs for *Calathea crotalifera*.

Construction		Model	Parameter
Density-independent environmentally stochastic IPM		$n(z', t+1) = \int_{\alpha}^{\omega} K(z',z,\psi_t)n(z,t)dz$	$\alpha = 0.57$ $\omega = 11.9$ z = leaf area
		$\psi_t = \{j_t, A_t\}$	ψ = an array containing climate values
K-kernel		$K(z',z,\psi_t) = P(z',z,j_t,A_t) + F(z',z,j_t)$	
Sub-kernels	**P**-kernel	$P(z',z,j_t,A_t) = s(z,j_t) * g(z',z,j_t,A_t)$	
	F-kernel	$F(z',z,j_t) = r_p(z,j_t) * r_o(z,j_t) * n_f * n_s * s_s(j_t)$ $* sdl_s(j_t) * sdl_{size}(z',j_t)$	$n_f = 23$ $n_s = 3$
Demographic functions	Survival	$\text{logit}(s(z,\psi_t)) = s_i + s_z * z + s_j * j_t + s_{z*j} * z * j_t$	$s_i = -2.74$ $s_z = 0.95$ $s_j = 0.07$ $s_{z*j} = -0.02$
	Growth	$g(z',z,j_t,A_t) = \text{dnorm}(z', g_\mu(z,j_t,A_t), g_{sd})$	$g_{sd} = 1.53$
		$g_\mu(z,j_t,A_t) = g_i + g_z * z + g_j * j_t + g_A * A_t$ $+ g_{z*j} * z * j_t + g_{z*A} * z * A_t$ $+ g_{j*A} * j_t * A_t + g_{z*j*A} * z * j_t$ $* A_t$	$g_i = 0.76$ $g_z = 0.9$ $g_j = 0.03$ $g_A = 0.006$ $g_{z*j} = -0.001$ $g_{z*A} = 0.00045$ $g_{j*A} = -0.0052$ $g_{z*j*A} = 0.00035$
	Reproduction	$\text{logit}(r_p(z,j_t)) = r_{p,i} + r_{p,z} * z + r_{p,j} * j_t + r_{p,z*j}$ $* z * j_t$	$r_{p,i} = -13.23$ $r_{p,z} = 1.401$ $r_{p,j} = -0.213$ $r_{p,z*j} = 0.043$
		$r_o(z,j_t) = \exp(r_{o,i} + r_{o,z} * z + r_{o,j} * j_t + r_{o,z*j} * z$ $* j_t)$	$r_{o,i} = -6.673$ $r_{o,z} = 0.829$ $r_{o,j} = 0.067$ $r_{o,z*j} = -0.007$
		$s_s(j_t < 6) = 0.29$ $s_s(j_t \geq 6) = 0.32$	
		$sdl_s(j_t < 6) = 0.14$ $sdl_s(j_t \geq 6) = 0.95$	
		$sdl_{size}(z',j_t < 6) = \text{dnorm}(z', 3.08, 0.54)$ $sdl_{size}(z',j_t \geq 6) = \text{dnorm}(z', 2.88, 1.4)$	
Environment values	Canopy openness*	$j \sim N(3, 1.4)$	
	Photosynthetic rate*	$A \sim N(6, 0.8)$	

* In Westerband and Horvitz (2017), canopy openness (j) and photosynthetic rate (A) were modelled as random samples from a sequence of values or draws from a uniform distribution. Specifically canopy openness was realized at time t as random draws from the sequence $\{1, 2, 3, 4, 5\}$ whilst photosynthetic rate was realized at time t as random draws from a uniform distruction (*i.e.*, $A \sim U(5, 7)$). However, since our manipulation of the environment involves explicitly changing the temporal variance of a series, we coerced the distributions into normal distributions with the same mean and reported variance of the original sampling distributions reported in Westerband and Horvitz (2017).

765 **Supplementary Table 3: Formulas, regressions and parameters used to construct the**
766 **IPMs for *Carlina vulgaris*.**
767

Construction		Model	Parameter
Density-independent environmentally stochastic IPM		$n(z', t+1) = \int_{\alpha}^{\omega} K(z', z, \psi_t) n(z,t) dz$	$\alpha = 1.5$ $\omega = 5$ $z = \log($longest leaf length$)$ $\psi_t =$ an array containing the parameters associated with environmentally stochastic demographic functions
K-kernel		$K(z', z, \psi_t) = P(z', z, \psi_t) + F(z', z, \psi_t)$	
Sub-kernels	**P**-subkernel	$P(z', z, \psi_t) = p_s(z, \psi_t) * [1 - p_f(z)] * g(z', z, \psi_t)$	
	F-subkernel	$F(z', z, \psi_t) = p_s(z, \psi_t) * p_f(z, \psi_t) * f_n(z)$ $* f_d(z', \psi_t) * p_e$	$p_e = 0.00095$
Demographic functions	Size dynamics: Rosette growth and recruit size	$g(z', z, \psi_t) = \text{dnorm}(z', g_\mu(z, \psi_t), g_{sd})$ $g_\mu(z, \psi_t) = g_{i,t} + g_{z,t}(z)$ $f_{d,t} = \text{dnorm}(z', f_\mu, f_{sd})$	$g_{sd} = 0.29$ $g_i, r_\mu \sim \text{MVN}(\mu, \Sigma)$ $\mu = (1.14, 3.16)$ $\Sigma = \begin{pmatrix} 0.037 & 0.041 \\ 0.041 & 0.075 \end{pmatrix}$ $g_z \sim \text{N}(0.74, 0.13)$ $f_{sd} = 0.5$
	Probability of survival	$\text{logit}(p_s(z, \psi_t)) = s_i + s_z * z$	$s_i \sim \text{N}(-2.28, 1.16)$ $s_z \sim \text{N}(0.90, 0.41)$
	Probability of flowering	$\text{logit}(fl_p(z, \psi_t)) = fl_i + fl_z * z$	$fl_i \sim \text{N}(-16.19, 1.03)$ $fl_z = 3.88$
	Seed production	$f_n(z) = \exp(A + B * z)$	$A = 1, B = 2$

768

769

770

771

772

773

774

775

776

777

Supplementary Table 4: Formulas, regressions and parameters used to construct the
IPMs for *Heliconia tortuosa*.

Construction		Model	Parameter
Density-independent environmentally stochastic IPM		$n(z', t+1) = \int_\alpha^\omega K(z', z, \psi_t) n(z,t) dz$	$\alpha = 0.78$ $\omega = 11.07$ z = leaf area
		$\psi_t = \{j_t, A_t\}$	ψ = an array containing climate values
K-kernel		$K(z', z, \psi_t) = P(z', z, j_t, A_t) + F(z', z, j_t)$	
Sub-kernels	**P**-kernel	$P(z', z, j_t, A_t) = s(z, j_t) * g(z', z, j_t, A_t)$	
	F-kernel	$F(z', z, j_t) = r_p(z, j_t) * r_o(z, j_t) * n_f * n_s * s_s(j_t)$ $* sdl_s(j_t) * sdl_{size}(z', j_t)$	$n_f = 37$ $n_s = 2.5$
Demographic functions	Survival	$\text{logit}(s(z, \psi_t)) = s_i + s_z * z + s_j * j_t + s_{z*j} * z * j_t$	$s_i = -2.05$ $s_z = 0.78$ $s_j = -0.22$ $s_{z*j} = 0.05$
	Growth	$g(z', z, j_t, A_t) = \text{dnorm}(z', g_\mu(z, j_t, A_t), g_{sd})$	$g_{sd} = 0.71$
		$g_\mu(z, j_t, A_t) = g_i + g_z * z + g_j * j_t + g_A * A_t$ $+ g_{z*j} * z * j_t + g_{z*A} * z * A_t$ $+ g_{j*A} * j_t * A_t + g_{z*j*A} * z * j_t$ $* A_t$	$g_i = 2.6$ $g_z = 0.56$ $g_j = -1.55$ $g_A = 0.44$ $g_{z*j} = 0.18$ $g_{z*A} = -0.034$ $g_{j*A} = 0.014$ $g_{z*j*A} = -0.0014$
	Reproduction	$\text{logit}(r_p(z, j_t)) = r_{p,i} + r_{p,z} * z + r_{p,j} * j_t + r_{p,z*j}$ $* z * j_t$	$r_{p,i} = -12.55$ $r_{p,z} = 1.527$ $r_{p,j} = 0.154$ $r_{p,z*j} = -0.013$
		$r_o(z, j_t) = \exp(r_{o,i} + r_{o,z} * z + r_{o,j} * j_t + r_{o,z*j} * z$ $* j_t)$	$r_{o,i} = -1.009$ $r_{o,z} = 0.157$ $r_{o,j} = -0.382$ $r_{o,z*j} = 0.048$
		$s_s(j_t < 6) = 0.15$ $s_s(j_t \geq 6) = 0.2$	
		$sdl_s(j_t < 6) = 0.26$ $sdl_s(j_t \geq 6) = 0.33$	
		$sdl_{size}(z', j_t < 6) = \text{dnorm}(z', 2.73, 0.71)$ $sdl_{size}(z', j_t \geq 6) = \text{dnorm}(z', 2.34, 1.17)$	
Environment values	Canopy openness	$j \sim N(3, 1.4)$	
	Photosynthetic rate	$A \sim N(6.5, 0.8654937)$	

* In Westerband and Horvitz (2017), canopy openness (j) and photosynthetic rate (A) were modelled as random samples from a sequence of values or draws from a uniform distribution. Specifically canopy openness was realized at time t as random draws from the sequence $\{1, 2, 3, 4, 5\}$ whilst photosynthetic rate was realized at time t as random draws from a uniform distruction (*i.e.*, $A \sim U(5, 8)$). However, since our manipulation of the environment involves explicitly changing the temporal variance of a series, we coerced the distributions into normal distributions with the same mean and reported variance of the original sampling distributions reported in Westerband and Horvitz (2017).